Experimental Hematology

Experimental Hematology 2019;70:42–54

CircPAN3 mediates drug resistance in acute myeloid leukemia through the miR-153-5p/miR-183-5p–XIAP axis

Jin Shang[a], Wei-Min Chen[a], Zhi-Hong Wang[a], Tian-Nan Wei[a], Zhi-Zhong Chen[b], and Wen-Bing Wu[b]

[a]*Provincial Clinical Medical College of Fujian Medical University; Department of Hematology, Fujian Provincial Hospital, Fuzhou, Fujian, China;* [b]*Department of Pathology, Fujian Provincial Hospital; Provincial Clinical Medical College of Fujian Medical University, Fuzhou, Fujian, China*

(Received 17 July 2018; revised 19 October 2018; accepted 30 October 2018)

The contribution and role of circular RNAs (circRNAs) in mediating chemoresistance in acute myeloid leukemia (AML) are still poorly understood and need further investigation. In this study, we established a doxorubicin (ADM)-resistant THP-1 AML cell line (THP-1/ADM). A high-throughput microarray was used to identify circRNA expression profiles of THP-1/ADM cells and naive THP-1 cells. The identified potential functional circRNA molecule was further validated in THP-1/ADM cells and bone marrow (BM) specimens from 42 AML patients. The interactions with target microRNAs (miRNAs) and downstream messenger RNAs (mRNAs) were also explored. As a result, 49 circRNAs that are significantly differentially expressed between THP-1/ADM and THP-1 cells were identified. Of these circRNAs, downregulation of circPAN3 by small interfering RNA significantly restored ADM sensitivity of THP-1/ADM cells. Furthermore, BM samples from patients with refractory and recurrent AML showed increased expression of circPAN3. A detailed circRNA/miRNA/mRNA interaction network was predicated for this circRNA. Subsequent mechanistic experiments showed that downregulation of circPAN3 could decrease the expression of X-linked inhibitor of apoptosis protein (XIAP), but this effect was counteracted by miR-153-3p or miR-183-5p specific inhibitors. Luciferase experiments further demonstrated that these molecules are involved in the circPAN3 regulatory network. Our results revealed that circPAN3 may be a key mediator for chemoresistance of AML cells, which may depend on the circPAN3–miR-153-5p/miR-183-5p–XIAP axis. Our findings provide evidence that circPAN3 can be a valuable indicator for predicting clinical efficacy of chemotherapy in AML patients and also can serve as a potential target for reversing drug resistance in AML. © 2018 Published by Elsevier Inc. on behalf of ISEH – Society for Hematology and Stem Cells.

Acute myeloid leukemia (AML) is one of the most common hematological malignancies [1,2]. Despite the application of new molecular targeted drugs and progress of allogeneic hematopoietic stem cell transplantation, chemoradiotherapy is still the mainstay for the treatment of AML. However, AML cells are demonstrated to unavoidably develop primary or secondary chemoresistance, thereby resulting in refractory and recurrent disease in patients. So far, most clinical trials of chemotherapy have shown very limited benefits for refractory and recurrent AML [3]. Therefore, it is necessary to identify the potential molecular targets and novel pathways underlying the occurrence and development of AML drug resistance.

Development of drug resistance in cancer cells involves interactions among multiple genes and signaling pathways. Currently, the mechanisms of drug resistance in AML include ATP-binding cassette (ABC) transporter-mediated multidrug resistance, apoptosis tolerance, FLT3 mutation, DNA repair abnormalities, and the bone marrow (BM) microenvironment [4]. In

Offprint requests to: Wei-Ming Chen, M.D., Professor of Medicine, Provincial Clinical Medical College of Fujian Medical University, Department of Hematology, Fujian Provincial Hospital, 134 Dong Jie Road, Fuzhou 350001, Fujian, China; E-mail: chenwm1962@163.com

Supplemental material associated with this article can be found, in the online version, at 10.1016/j.exphem.2018.10.011.

0301-472X/
https://doi.org/10.1016/j.exphem.2018.10.011

addition to these mechanisms, growing evidence shows that noncoding RNAs (ncRNAs) are associated with drug resistance in some solid tumors [5], leading to more attention being focused on targeting ncRNAs as a new strategy for overcoming multidrug resistance of cancer.

ncRNAs, generally classified as transcribed ultraconserved regions, microRNAs (miRNAs), small nucleolar RNAs, PIWI-interacting RNAs, long noncoding RNAs, and circular RNAs (circRNAs) account for almost 95% of the total RNAs transcribed from eukaryotic genomes and are being increasingly recognized to function in gene regulation and to contribute to the pathogenesis of various human disorders [6]. As a large proportion of the ncRNA family, circRNAs have attracted growing interest in recent years. circRNAs have been recognized as a class of molecules with variable biological functions. They can compete for the pool of the same miRNA response elements (MREs) to influence the activities of miRNAs in the regulation of gene expression [7]. With the structure of covalently closed continuous loop without 5′ to 3′ polarity and polyadenylated tail, circRNAs show a higher stability than linear transcripts and are not affected by ribonuclease R or RNA exonuclease [8]. Furthermore, circRNAs exhibit evolutionary conservation as well as tissue and developmental stage specificity [9,10], thereby suggesting their important role in mediating gene expression variability. With the development of high-throughput sequencing, aberrant expression of circRNAs has been found in a wide range of solid tumors [11–16] and is associated with tumor differentiation, invasion, and distant metastasis [13,14]. In some solid tumors, circRNAs have been reported to be involved in the development of chemo- and radioresistance of tumor cells [15,17]. However, the functional role of circRNAs in chemoresistance of AML and the underlying mechanism have been studied only rarely.

In this study, using high-throughput circRNA microarray, we compared the expression profile of circRNAs in chemosensitive and chemoresistant AML cells. An important circRNA molecule, circPAN3, was identified to play a crucial role in driving drug resistance of AML and the underlying interaction network and downstream functional components were also investigated for this molecule.

Materials and Methods

Cell culture and collection of human samples

THP-1 human AML cells were purchased from the American Type Culture Collection (ATCC, Manassas, VA, USA) and cultured in Dulbecco's modified Eagle's medium with 10% fetal bovine serum (Thermo Fisher Scientific Inc., Waltham, MA, USA). A doxorubicin (ADM)-resistant cell line (THP-1/ADM) was established by exposing THP-1 cells to a gradually increasing concentration (0.2–2 μg/mL) of ADM for 6 months. The untreated parental cell line was used as a control.

BM samples were obtained from 42 AML patients who were hospitalized at Fujian Provincial Hospital (Fuzhou, China) between May 2015 and May 2018. Briefly, mononuclear cells were isolated from BM aspirates by density gradient centrifugation using Ficoll-Paque Plus density gradient media (Pharmacia LKB Biotechnology, Piscataway, NY, USA). Two million cells were collected from each sample for further examination.

The patient population consisted of 22 males and 20 females with a median age of 31. Of these patients, 22 (52.4%) had newly diagnosed AML and responded well to chemotherapy, whereas the rest ($n = 20$, 47.6%) had refractory/recurrent AML and responded poorly to chemotherapy. Pathological diagnosis and confirmation of recurrence and refractoriness of AML were defined according to the published criteria [18]. The study was conducted in accordance with the Declaration of Helsinki and the protocol was approved by the ethics committee of Fujian Provincial Hospital. All patients provided written informed consent before participation.

Assessment of cell sensitivity to ADM

Cell Count Kit-8 (CCK-8) reagent (Vazyme Biotech, Nanjing, China) was used to assess cell sensitivity to ADM. THP-1/ADM and THP-1 cells were plated in 96-well plates at a density of 1×10^4 cells/mL and then treated with 200 μL of medium containing various concentrations of ADM (0.01–2.4 μg/mL) for 24 hours. Next, 10 μL of CCK-8 reagent was added to cultured cells, and incubated in a humidified incubator containing 5% CO_2 at 37°C for 2 hours. Absorbance was detected at a wavelength of 450 nm. The half-maximal inhibitory concentration (IC_{50}) and inhibitory ratio values were calculated from the concentration–response curve generated for each cell line.

Expression profile analysis of circRNAs

A circRNA chip (Arraystar Human Circular RNA Microarray, ArrayStar, Rockville, MD, USA) containing 13617 probes specific for human circRNA splicing sites and Agilent Scanner G2505C (Agilent Technologies Inc., Santa Clara, CA, USA) were used for analyzing circRNA expression profiles of THP-1 and THP-1/ADM cell lines. Specifically, three pairs of samples (THP-1 and THP-1/ADM cells) were analyzed on the chips following hybridization and washing. Exogenous RNAs developed by the External RNA Controls Consortium (ERCC, Stanford, CA, USA) were used as controls. Scanned images were imported into Agilent Feature Extraction software (version 11.0, Agilent Technologies Inc.) for raw data extraction. Quantile normalization and subsequent data processing were performed using the R software package. Those with fold change ≥2.0 and a p value < 0.05 were selected as differentially expressed circRNAs with statistical significance.

Quantitative real-time polymerase chain reaction

Total RNA was extracted from cell lines and BM tissue samples using TRIzol reagent and reversely transcribed into cDNA using MLV RTase cDNA Synthesis Kit (Takara Bio

Table 1. Primers used for qRT-PCR of the top 10 upregulated circRNAs

circRNA	Gene Symbol	Forward Primer Sequence (5′–3′)	Reverse Primer Sequence (5′–3′)
hsa_circ_0100989	*GPC5*	CAGCCTCCCTCAGCACTACT	TTATGAGCGTTTTCCCTCTGA
hsa_circ_0102446	*GPHN*	CAGCCTCCCTCAGCACTACT	TTATGAGCGTTTTCCCTCTGA
hsa_circ_0100181	*PAN3*	GATTTCCATGCTGGAGGAGA	GGAATGAAGAGGGGAAGACC
hsa_circ_0101868	*PRPF39*	ATGAGCAGGGAAACCTGAGA	TCTGAACTGTTGCCTGTGCT
hsa_circ_0104204	*CSNK1G1*	ACTCCAATGCACCAATCACA	GTTGCCATCTCCTCTGGAAA
hsa_circ_0001264	*RAD18*	CAGCTCATTAAAAGGCACCA	GGAAGAAGCAGGAGATTTGG
hsa_circ_0102888	*PP4R3A*	ATGGATCCCGCTACAATCTG	TGCCCATGTTTGACAAAGTC
hsa_circ_0100759	*DIAPH3*	CATCTTCCTGATCAAGAGCAATTA	GGGACAAAGGATCAATGGAA
hsa_circ_0101113	*FARP1*	GAGGAAGAGGAGGAGGTCGT	TGCGTCTTGCTGAGGTATGT
hsa_circ_0100891	*MYCBP2*	AATTGGACTCCAGGGGCTAT	TGGTAAATTTCCCTCAAGTGC

Inc., Kusatsu, Japan). Quantitative real-time polymerase chain reaction (qRT-PCR) was conducted with a LightCycler 480II RT-PCR system (Roche Applied Science, Indianapolis, IN, USA) according to the manufacturer's instructions. The reaction condition was 45 cycles of denaturation at 95°C for 15 sec, annealing at 60°C for 30 sec, and extension at 72°C for 10 sec. U6 RNA served as internal control. The circRNA sequences were obtained from circBase (www.circbase.org). The primers used in this study were listed in Table 1. The delta-delta cycle threshold (ΔΔCt) method was used for quantification [19].

Cell transfection

The small interfering RNA (siRNA) targeting the junction region of circPAN3 sequence (siRNA sequence: 5′-UCU GAC CCA AAA CAA CCC CdTdT-3′) and negative control siRNA (NC), as well as the mimics and inhibitors of miR-153-5p and miR-183-5p, were provided by Geneseed Bio-Tech (Guangzhou, China). Hieff Trans Liposomal Transfection Reagent (Yeasen Bio, Shanghai, China) was used for transfection. Briefly, THP-1 and THP-1/ADM cells, as well as leukemic cells from five relapsed AML patients, were cultured in six-well plates and transfected with the aforementioned siRNAs or miRNA mimics or inhibitors (10 nmol/well) for 6 h. The transfected cells were cultured in regular medium for 48 hours and then collected for subsequent experiments.

Prediction for the circRNA–miRNA–mRNA interaction network

The circRNA–miRNA interaction was predicted using Arraystar's homemade miRNA target prediction software based on TargetScan and miRanda. Cytoscape was applied to build a circRNA–miRNA–messenger RNA (mRNA)/gene interaction network. The predicted gene functions in the network were annotated using Gene Oncology (GO) and Kyoto Encyclopedia of Genes and Genomes (KEGG) pathway analysis.

Western blot analysis

Protein lysates from cell lines and BM tissue samples were subjected to Western blot analysis using the standard protocol as described previously [20]. Antibodies against X-linked inhibitor of apoptosis protein (XIAP) (catalog #AF6368, 1:500), pro-caspase 3 (pro-Cas-3, catalog #AF6311, 1:500), cleaved caspase 3 (CL Cas-3, catalog #AF7022, 1:500), pro-caspase 9 (pro-Cas-9, catalog #AF6348, 1:500), and cleaved-caspase 9 (CL Cas-9, catalog #AF5240, 1:500) were obtained from Affinity Biosciences (Changzhou, China). Antibody against β-actin (Affinity Biosciences, catalog #AF7018, 1:1000) was used as a loading control. Proteins were detected using Pierce ECL Western Blotting substrate (Thermo Fisher Scientific Inc.). The bands were quantified using Image-Pro Plus 6.0 software (Media Cybernetics, Rockville, MD, USA).

Luciferase assay

The wild-type (WT) and mutant sequences of circPAN3 and the 3′-untranslated region (3′-UTR) of *XIAP* were obtained through whole-genome synthesis. For the mutant sequences of circPAN3 and *XIAP* 3′-UTR, the putative binding sites for miR-153-5p and miR-183-5p were mutated (Supplementary Figures E1A and E1B, online only, available at www.exphem.org). All sequences were cloned into the XhoI and NotI sites of psiCHECK2 vector (Geneseed Bio-Tech) to construct the corresponding luciferase reporters (psiCHECK2/circPAN3, psiCHECK2/circPAN3-mut153, and psiCHECK2/circPAN3-mut183; psiCHECK2/XIAP 3′-UTR, psiCHECK2/XIAP 3′-UTR-mut153, and psiCHECK2/XIAP 3′-UTR-mut183) for transfection in 293T cells. Briefly, 3×10^4 293T cells were seeded in 24-well plates at 60% confluence level in triplicate and cotransfected with each of the indicated luciferase reporters (0.5 μg) and either miRNA mimics or NC. Forty-eight hours after cotransfection, the luciferase reporter assay was conducted using the Dual-Luciferase Reporter Assay System (Promega, Madison, WI, USA) according to the manufacturer's instructions. Relative luciferase activity was normalized to the Renilla luciferase internal control.

Statistical analysis

The Wilcoxon signed-rank test was performed to analyze significant differences regarding the expression level of circRNAs and miRNAs between samples. Pearson's analysis was applied to determine correlation coefficients for different variables. Other data are presented as means ± standard deviation (SD) and the Student *t* test (two-tailed) was performed for data analysis. $p < 0.05$ was considered to be significant.

Results

Verification of ADM-resistant THP-1 cell line

An ADM-resistant THP-1 cell line (THP-1/ADM) was established by continuous exposure to increasing

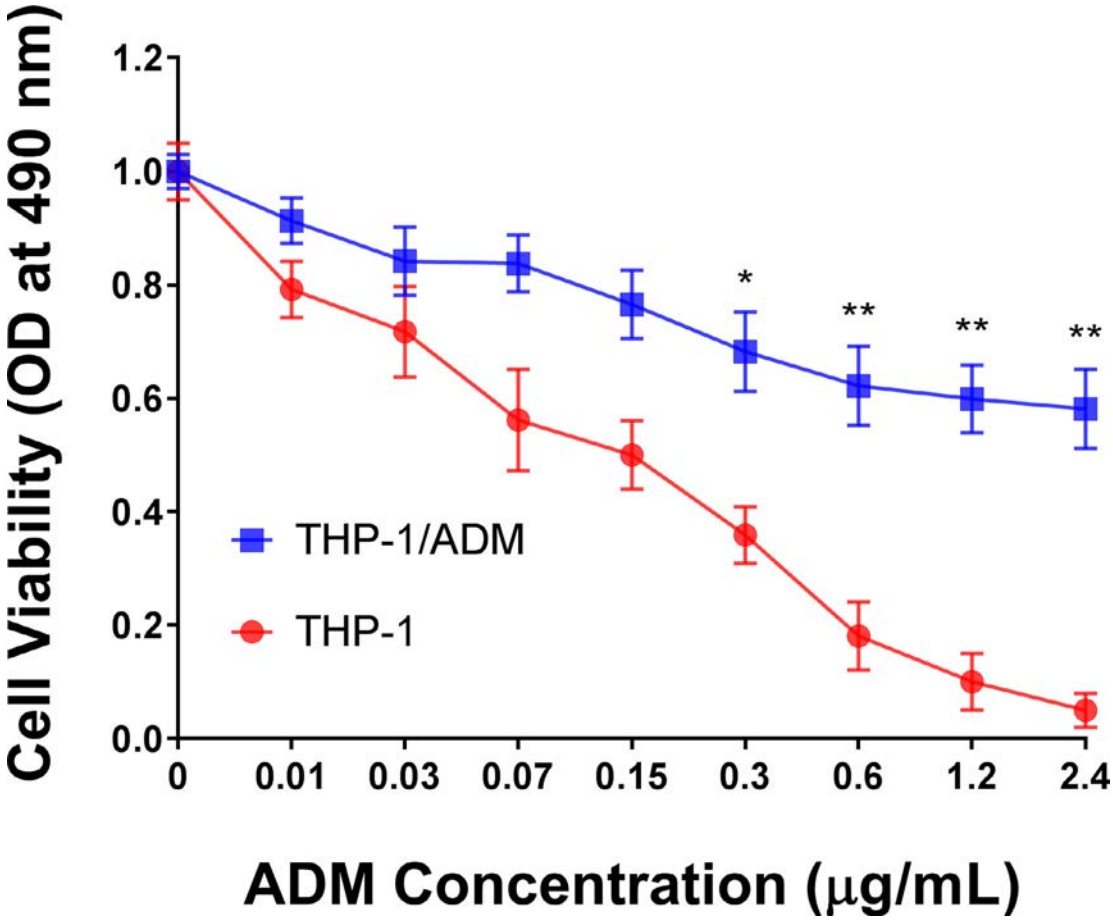

Figure 1. Comparison of sensitivity to ADM between THP-1 and THP-1/ADM cells. Data are presented as means ± SD ($n = 5$). *$p < 0.05$ and **$p < 0.01$.

concentrations of ADM for 6 months. To verify resistance, both drug-naive and drug-resistant THP-1 cells were treated with various concentrations of ADM for 24 hours and then the IC_{50} values were determined. As depicted in Figure 1, naive THP-1 cells had an IC_{50} value of 0.15 ± 0.05 μg/mL in response to ADM, whereas THP-1/ADM cells had an IC_{50} value of 2.62 ± 0.83 μg/mL, which was 17.5-fold higher than that of naive THP-1 cells. These results demonstrate the resistance to ADM in THP-1/ADM cell line.

Identification of differential circRNA expression profiles between ADM-naive and ADM-resistant THP-1 cells

Next, the circRNA expression profiles of naive and ADM-resistant THP-1 cells were analyzed using Arraystar Human circRNA Array. After normalization, a total of 4573 circRNA targets were identified in three pairs of THP-1 and THP-1/ADM cell samples. Differentially expressed circRNAs were displayed through fold change filtering (Figure 2A) and those with a statistically significant change in expression between the two groups were identified by a volcano plot (Figure 2B). As a result, 49 distinct circRNAs were found to be differentially expressed in the two cell lines with a fold change >2 and a p value < 0.05. Of these circRNAs, 35 were upregulated and 14 were downregulated in THP-1/ADM cells. The top 10 upregulated and downregulated circRNAs are listed in Table 2. In addition, the heat map of the top 50 upregulated and downregulated circRNAs further revealed distinctive circRNA expression pattern between THP-1 and THP-1/ADM cells (Figure 2C). Taken together, these data indicate that the expression of circRNAs in ADM-resistant AML cells is considerably different from that in naive cells, suggesting a potential role of circRNAs in conveying drug resistance in AML cells.

To validate the microarray analysis, we performed qRT-PCR for the top 10 upregulated circRNAs in three pairs of THP-1 and THP-1/ADM cells. As shown in Figures 2D and 2E, the log2 fold changes calculated for microarray data were highly correlated with those for qRT-PCR data (Pearson's $r = 0.682$, $p = 0.029$), thereby indicating overall consistency between microarray and qRT-PCR measurements.

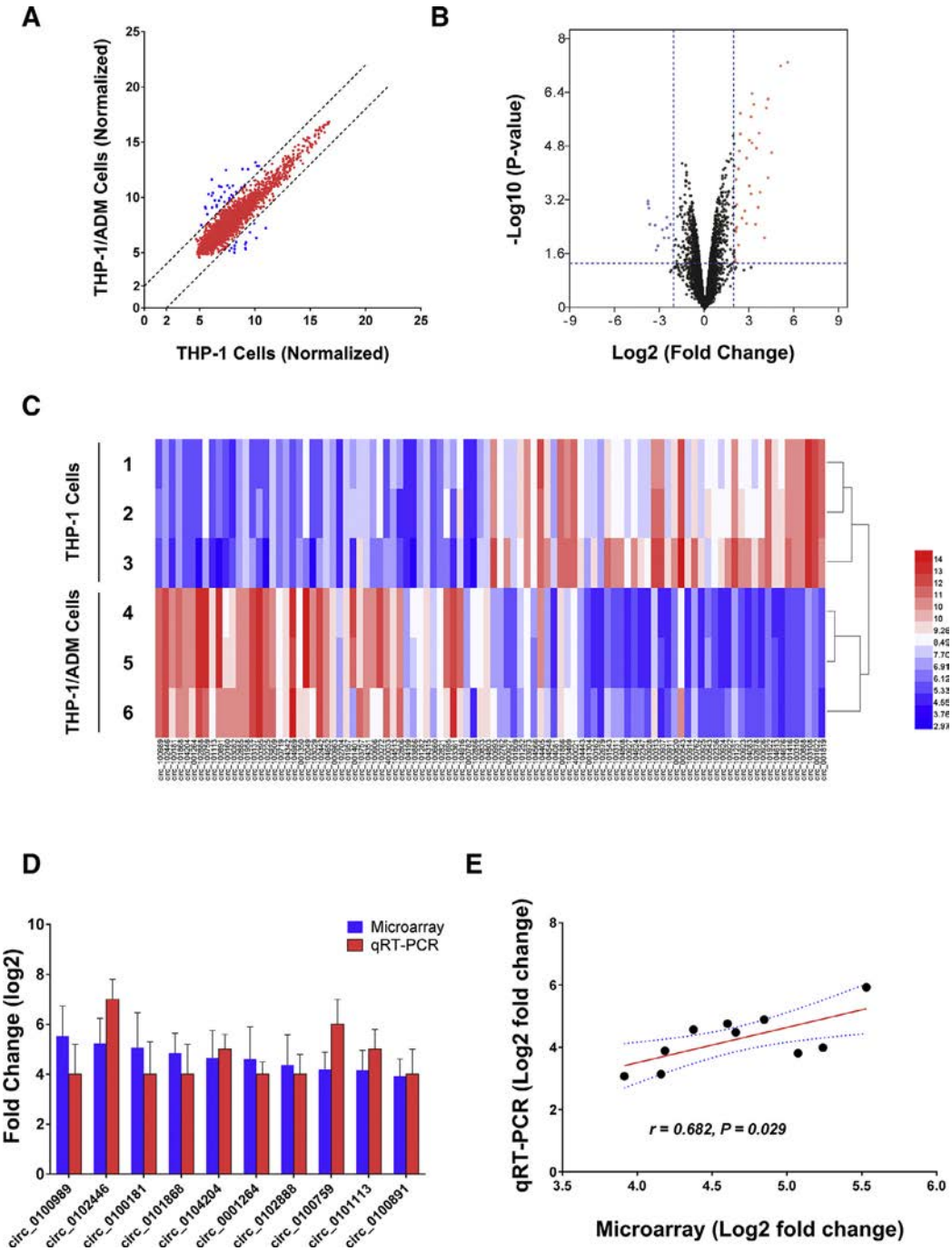

Figure 2. Characterization and comparison of circRNA expression profiles between THP-1 and THP-1/ADM cells. **(A)** Scatter plot evaluating the difference in circRNA expression profile. The values plotted on the X and Y axes represent the average normalized signals of each group (log2 scaled). Red dots between the two straight lines indicate the circRNAs showing no significant expression changes (<2.0-fold change) between the two cell lines. Blue dots above or below the two lines indicate the circRNAs showing >2.0-fold expression changes between the two types of cells. **(B)** Volcano plot visualizing differential expression of circRNAs between the two cell lines. The vertical lines correspond to 2.0-fold (log2 scaled) up and down, respectively. The horizontal line represents a *p* value of 0.05 (−log10 scaled). **(C)** Heat map showing expression profiles of the top 50 most significantly different circRNAs (both upregulated and downregulated) between THP-1/ADM and THP-1 cells. Each row represents a sample and each column represents a circRNA. Red represents high relative expression and blue represents low relative expression. Each group contains three samples. **(D,E)** Validation of microarray data by qRT-PCR. Ten circRNAs differentially expressed between THP-1/ADM and THP-1 cells were examined. Histograms in **(D)** indicate the mean values of log2 fold change in circRNA expression (THP-1/ADM vs. THP-1 cells). **(E)** Pearson's correlation analysis showing a very high correlation between both values (red line represents the fitted curve, blue dotted lines represent 95% confidence intervals [CIs]). The results indicate that microarray data matched well with qRT-PCR data.

Table 2. Top 10 upregulated and downregulated circRNAs between THP-1/ADM and THP-1 cells screened by microarray

CircRNA ID	Chromosome	*p* value	Fold Change	Best Transcript	Gene Symbol
Top 10 upregulated circRNAs					
hsa_circ_0100989	Chr21	0.000000049	5.522634	NM_004466.5	*GPC5*
hsa_circ_0102446	Chr14	0.000000062	5.095632	NM_020806	*GPHN*
hsa_circ_0100181	Chr13	0.000024300	4.483257	NM_175854	*PAN3*
hsa_circ_0101868	Chr14	0.000129000	4.239404	NM_017922.3	*PRPF39*
hsa_circ_0104204	Chr15	0.000000597	4.219353	NM_022048	*CSNK1G1*
hsa_circ_0001264	Chr3	0.000001100	4.086172	NM_020165	*RAD18*
hsa_circ_0102888	Chr14	0.008290000	3.993946	NM_001284281.1	*PP4R3A*
hsa_circ_0100759	Chr13	0.000352000	3.695359	NM_001042517.1	*DIAPH3*
hsa_circ_0101113	Chr13	0.000006200	3.635144	NM_001001715.3	*FARP1*
hsa_circ_0100891	Chr13	0.000985000	3.584472	NM_015057	*MYCBP2*
Top 10 downregulated circRNAs					
hsa_circ_0001819	Chr8	0.00064	−3.82166	NM_015902	*UBR5*
hsa_circ_0001622	Chr6	0.00078	−3.79373	NM_001137668	*CASP8AP2*
hsa_circ_0103108	Chr15	0.00109	−3.75534	NR_027992	*NBEAP1*
hsa_circ_0100888	Chr13	0.00313	−3.6837	NM_015057	*MYCBP2*
hsa_circ_0100310	Chr13	0.00341	−3.35805	NM_015032	*PDS5B*
hsa_circ_0101416	Chr14	0.01940	−3.25243	NR_027457	*LINC00221*
hsa_circ_0104676	Chr15	0.01430	−3.1281	NM_015629	*PRPF31*
hsa_circ_0104613	Chr15	0.00461	−2.82206	XM_011522038.1	*PEAK1*
hsa_circ_0101922	Chr14	0.00784	−2.71451	NM_172193.2	*KLHDC1*
hsa_circ_0100926	Chr13	0.00406	−2.52645	NM_001242868	*SLAIN1*

CircRNA ID was based on circBase (http://www.circbase.org/). *p* value was calculated from paired *t* test. Fold change represents the ratio (log scale) of normalized intensities between two cell lines.

Identification of circPAN3 in THP-1/ADM cells and clinic samples

Based on Table 2, we found that circPAN3 is in the top 10 upregulated target circRNAs. It has been reported that the gene *PAN3* is considered a candidate gene located in amplified chromosome regions in AML patients with a complex karyotype [21], whereas the findings of our circRNA expression analysis indicate that circPAN3 may be involved in the resistance to ADM of THP-1 cells. To verify this, we downregulated the expression of circPAN3 in THP-1/ADM cells using a targeted siRNA and then examined the sensitivity of the treated cells to ADM. As a result, we found that downregulation of circPAN3 by siRNA considerably increased the sensitivity of THP-1/ADM cells to ADM compared with the scrambled negative control ($IC_{50} = 0.32 \pm 0.06$ μg/mL and 2.41 ± 0.23 μg/mL in the si-circPAN3 and si-NC groups, respectively) (Figure 3A), thereby suggesting a role of circPAN3 in the development of drug resistance in AML cells. For further validation, we examined the expression of circPAN3 in BM samples from refractory/recurrent AML patients ($n = 20$) and those sensitive to chemotherapy ($n = 22$). As shown in Figure 3B, refractory/recurrent AML patients had a significantly higher expression level of circPAN3 in their BM than chemosensitive patients did ($p < 0.01$), which is further evidence that circPAN3 is most likely to contribute to postchemotherapy recurrence in AML patients.

Identification of the circRNA–miRNA interaction network for circPAN3

circRNAs usually act as an miRNA sponge and regulate their own circRNA–miRNA–mRNA networks [22]. To identify the circRNA–miRNA interaction network for circPAN3, we first analyzed the MREs associated with circPAN3 and predicted potential target miRNAs through TargetScan and miRanda. Then, we ranked the predicted target miRNAs of circPAN3 according to their mirSVR scores and the top 10 candidates (miR-153-5p, miR-183-5p, miR-338-3p, miR-346, miR-545-3p, miR-574-5p, miR-599, miR-653-5p, miR-766-3p, and miR-767-3p) were selected for further analysis. In brief, the bioinformatics tool DIANA was used to predict the target genes of these miRNAs, followed by function analysis of the predicted target genes by GO and KEGG. GO enrichment analysis revealed that these predicted target genes are involved in a wide range of cellular activities, such as cytosol, protein complex, biosynthetic process, and cellular nitrogen compound metabolic process (Supplementary Figure E2A, online only, available at www.exphem.org), whereas KEGG analysis showed that a few target genes are involved in several important signaling pathways associated with cancer development and progression such as the transforming growth factor-beta, mammalian target of rapamycin, ErbB, and FoxO signaling pathways (Supplementary Figure E2B, online only, available at www.exphem.org). Then, we focused

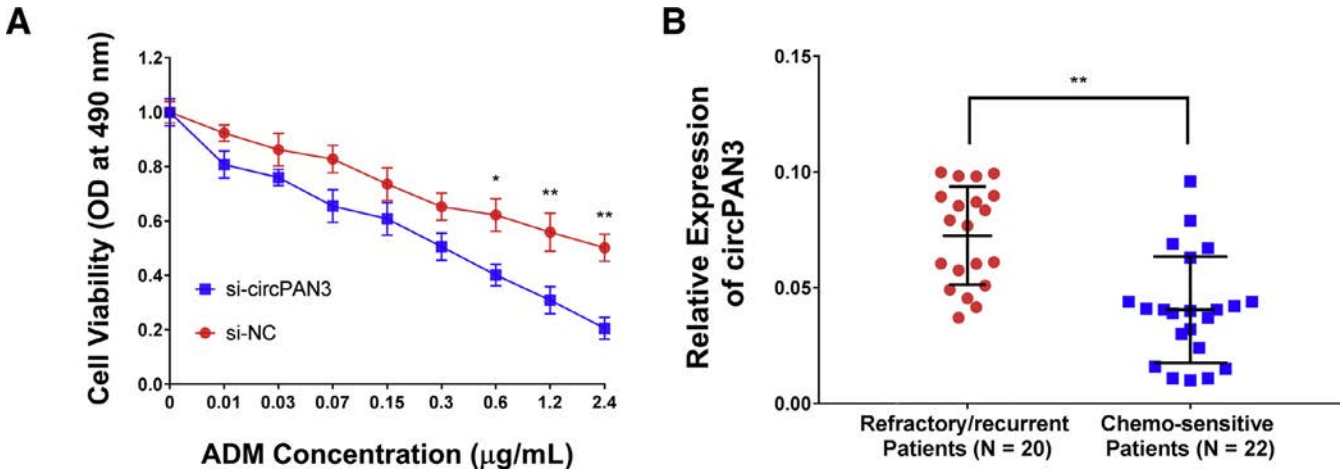

Figure 3. **(A)** Comparison of sensitivity to ADM between THP-1/ADM cells transfected with circPAN3 siRNA or the corresponding NC. Data are presented as means ± SD ($n = 5$). *$p < 0.05$ and **$p < 0.01$. **(B)** Comparison of expression of circPAN3 in BM tissues from refractory/recurrent AML patients ($n = 20$) and those sensitive to chemotherapy ($n = 22$). Refractory/recurrent AML patients had a significantly higher expression level of circPAN3 in their BM than chemosensitive patients did. **$p < 0.01$.

on the KEGG Pathways in Cancer, an important tumor-related pathway in KEGG database. It involved all 10 target miRNAs and 138 target genes of circPAN3 and had a significant p value of 0.01, suggesting an essential role of circPAN3 in cancer-related pathways for AML with the greatest potential. Next, we employed Cytoscape to construct the circRNA–miRNA–mRNA interaction network of circPAN3 within the KEGG Pathways in Cancer (Supplementary Figure E2C, online only, available at www.exphem.org).

circPAN3 functions in ADM resistance in THP-1/ADM cells through targeting XIAP

In the network shown in Supplementary Figure E2C (online only, available at www.exphem.org), XIAP was found to be targeted by both miR-153-5p and miR-183-5p, suggesting that it might be a crucial factor mediated by circPAN3. Overexpression of XIAP in AML has been demonstrated to lead to chemoresistance [23], whereas its downregulation induces activation of caspases and apoptosis of leukemic cells [24]. Considering the functions of XIAP and its connection with circPAN3, we therefore hypothesized that the circPAN3–miR-153-5p/miR-183-5p–XIAP axis may contribute to circPAN3-medicated ADM resistance in THP-1/ADM cells.

To validate our hypothesis, we first detected the mRNA and protein levels of XIAP in THP-1/ADM and THP-1 cell lines by qRT-PCR and Western blot. As shown in Figures 4A and 4B, the mRNA and protein levels of XIAP were significantly increased in ADM-resistant cells compared with naive cells. Furthermore, we examined the mRNA and protein expression of XIAP in BM samples from 20 refractory/recurrent AML patients and 22 chemosensitive AML patients. The results were consistent with those of the cell experiments, showing that the mRNA and protein levels of XIAP were dramatically higher in samples from refractory/recurrent patients than in those from chemosensitive patients (Figures 4C and 4D). Collectively, these data showed a significant association between XIAP and chemoresistance of AML.

Then, we treated the cells using circPAN3-specifc siRNA to downregulate the expression of circPAN3, which decreased by about 70% as validated by qRT-PCR. We found that the protein level of XIAP was also significantly decreased compared with the mock control (Figure 4F), but this was not the case for XIAP mRNA (Figure 4E). These findings indicated a post-transcriptional regulation mechanism of circPAN3 on XIAP. We also examined the clinical samples from all refractory/recurrent and chemosensitive AML patients and observed a significant positive correlation between circPAN3 level and XIAP protein level (Pearson's $r = 0.543$, $p = 0.0002$) (Figure 4G). These results, together with the data shown in Figure 3A, suggest that XIAP serves as a key molecule in circPAN3-mediated drug resistance in AML.

Determination of the regulatory role of circPAN3–miR-153-5p/miR-183-5p–XIAP axis

We further elucidated the role of the circPAN3–miR-153-5p/miR-183-5p–XIAP axis in drug resistance of THP-1/ADM cells. First, we treated THP-1/ADM cells with miR-153-5p and miR-183-5 mimics, respectively. As shown in Figure 5A, both mimics significantly decreased the protein expression of XIAP in THP-1/ADM cells, which demonstrates the effect of miR-153-5p and miR-183-5p on the expression of XIAP. When THP-1/ADM cells were cotransfected with circPAN3-specific siRNA and either miR-153-5p or miR-183-5p

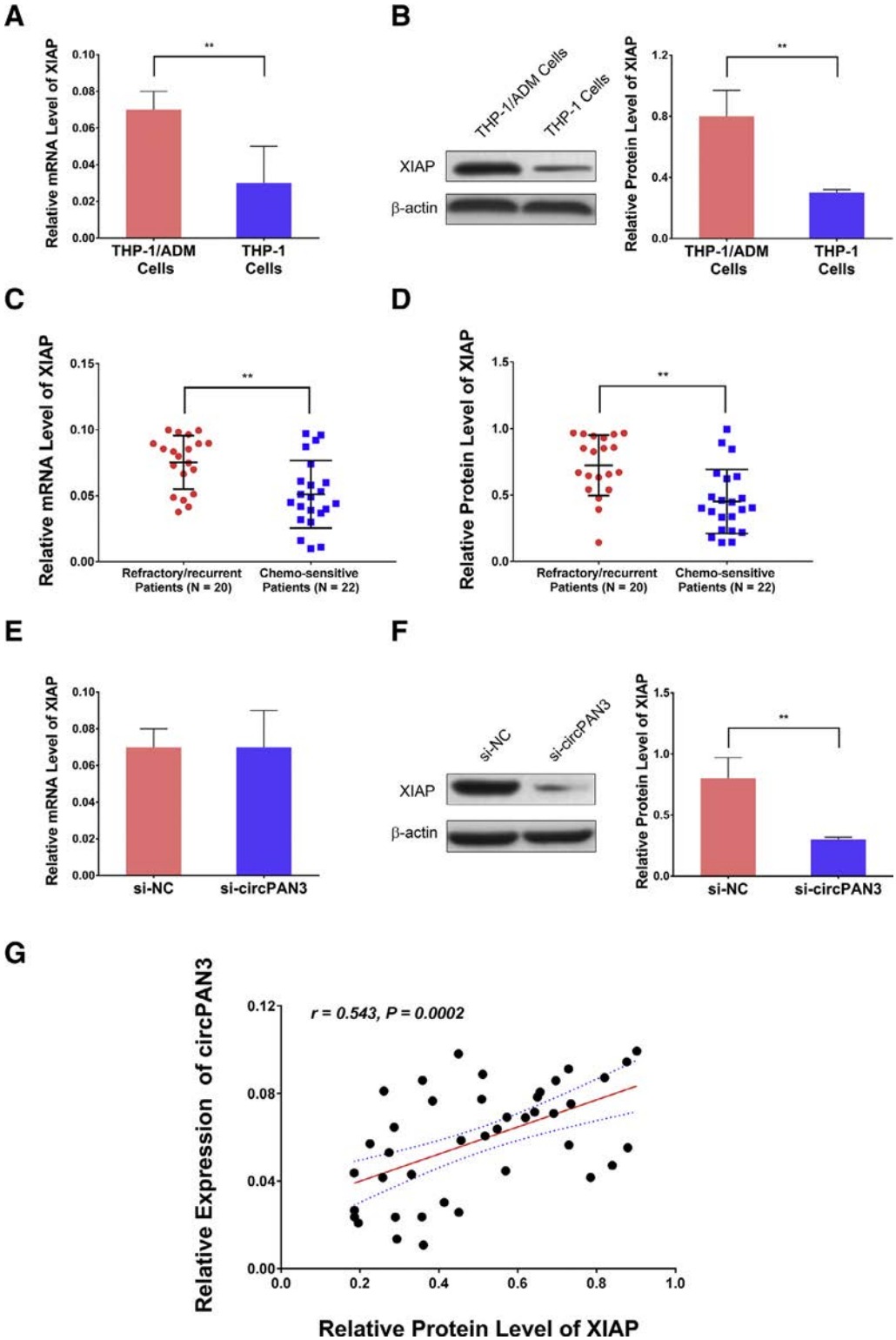

Figure 4. **(A,B)** mRNA and protein levels of XIAP in THP-1 and THP-1/ADM cells determined by qRT-PCR and Western blot analysis. Beta-actin served as an internal control. Data are presented as means ± SD ($n = 5$). $^{**}p < 0.01$. **(C,D)** mRNA and protein levels of XIAP in BM tissues from refractory/recurrent AML patients ($n = 20$) and those sensitive to chemotherapy ($n = 22$). $^{**}p < 0.01$. **(E,F)** mRNA and protein levels of XIAP in THP-1/ADM cells transfected with circPAN3 siRNA or the corresponding NC, which were determined by qRT-PCR and Western blot, respectively. Beta-actin served as an internal control. Data are presented as means ± SD ($n = 5$). $^{**}p < 0.01$. **(G)** Pearson's correlation analysis between circPAN3expression of XIAP protein expression in BM samples from all AML patients. A significant correlation could be observed (red line represents the fitted curve; blue dotted lines represent 95% confidence intervals [CIs]).

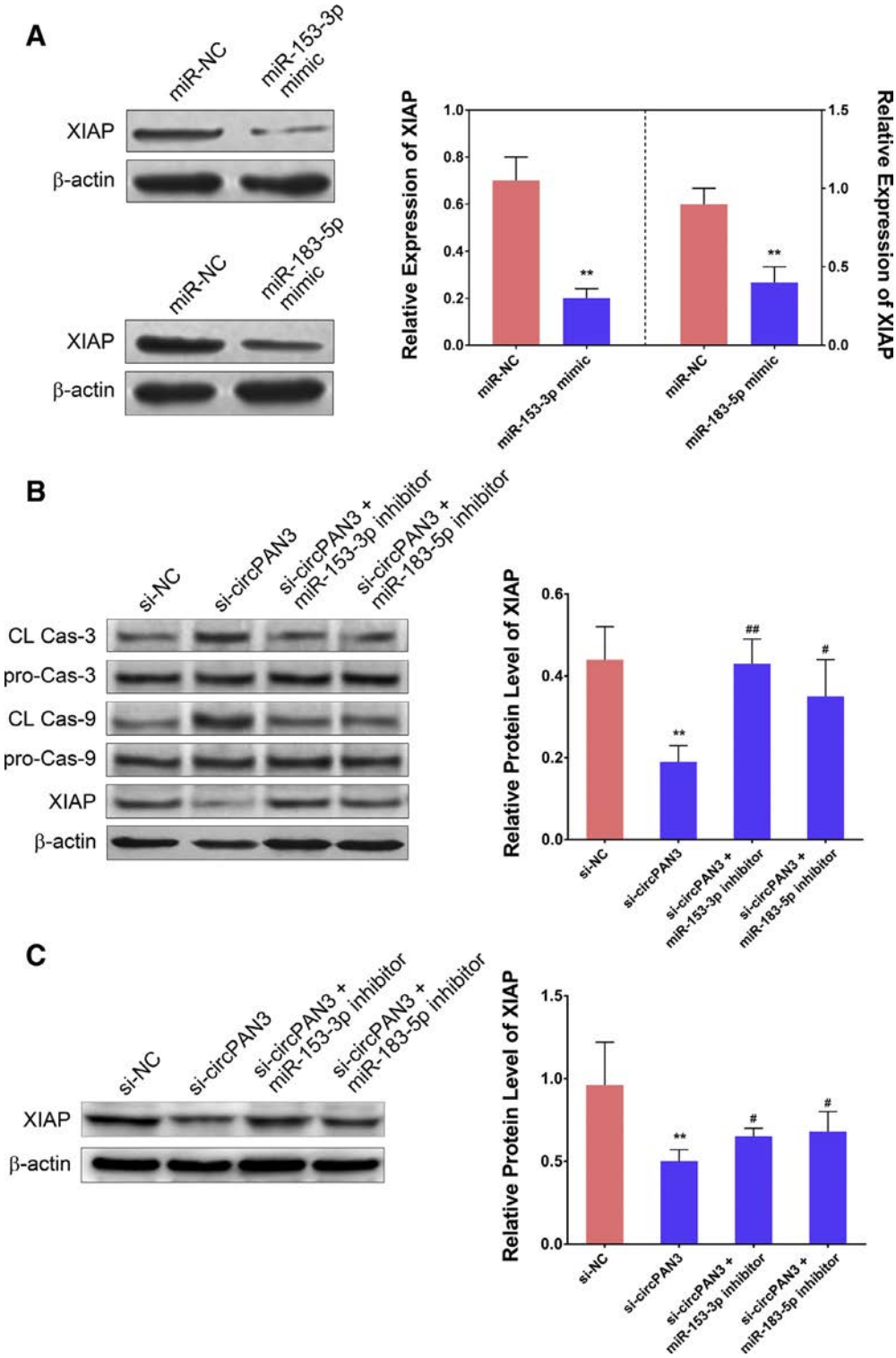

Figure 5. **(A)** miR-153-3p or miR-183-5p mimics could significantly decrease the protein level of XIAP in THP-1/ADM cells. The protein level of XIAP was determined by Western blot. Beta-actin served as an internal control. Data are presented as means ± SD ($n = 5$). $^{**}p < 0.01$ compared with miR-NC. **(B)** Effects of circPAN3 downregulation on XIAP expression and the ratios of CL Cas-3/pro-Cas-3 and CL Cas-9/pro-Cas-9 were blocked by specific inhibitors of miR-153-3p and miR-183-5p. The protein levels were determined by Western blot in THP-1/ADM cells cotransfected with circPAN3-specific siRNA and either miR-153-5p or miR-183-5p specific inhibitors. **(C)** In leukemic cells from five relapsed AML patients, the effect of circPAN3 downregulation on XIAP expression was also inhibited by miR-153-5p or miR-183-5p inhibitors. For **(B)** and **(C)**, β-actin served as an internal control. Data are presented as means ± SD ($n = 5$). $^{**}p < 0.01$ compared with miR-NC; $^{\#}p < 0.05$ and $^{\#\#}p < 0.01$ compared with si-circPAN3.

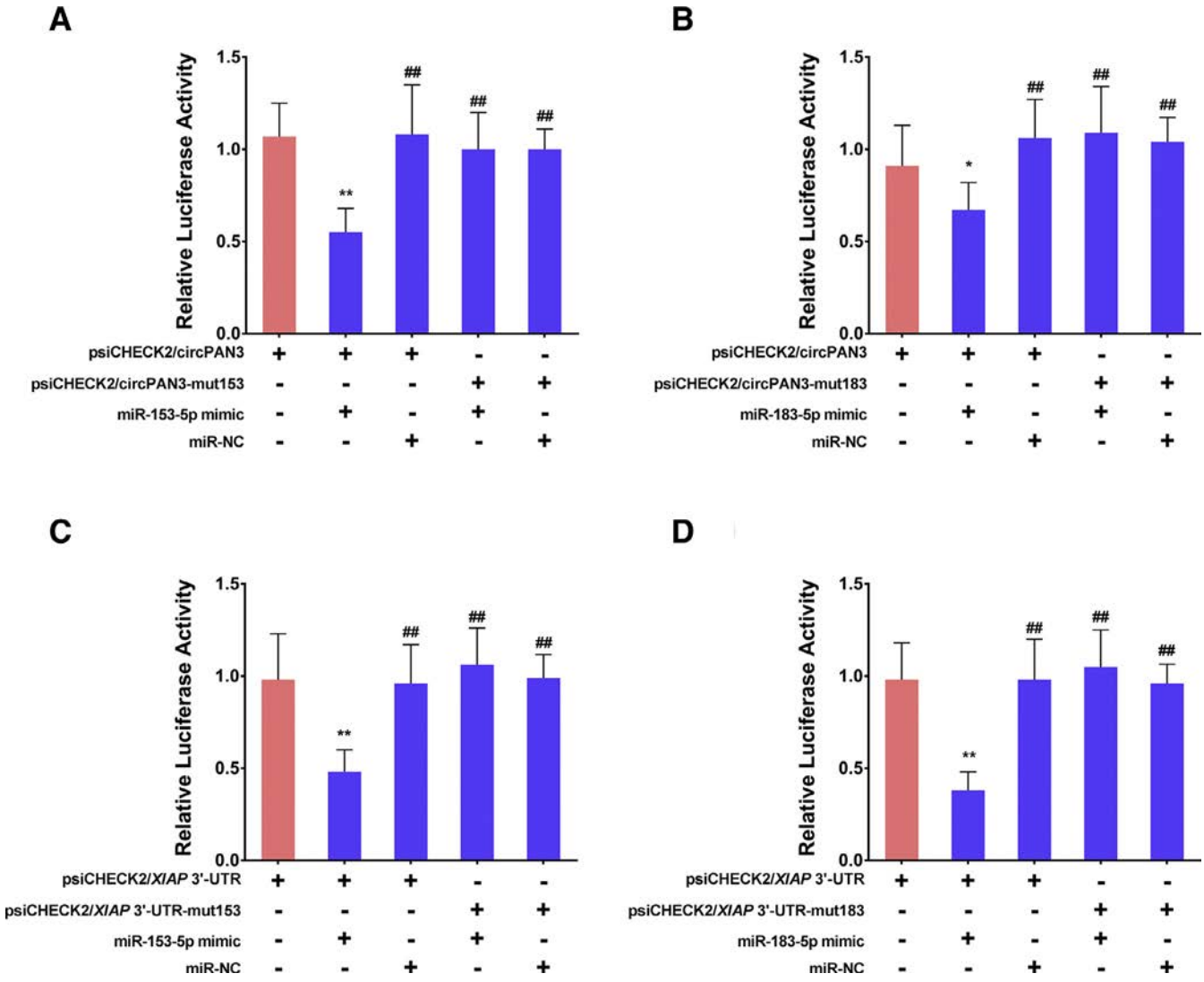

Figure 6. **(A,B)** Relative luciferase activities analyzed in 293T cells upon cotransfection of miR-153-5p mimic and luciferase reporter psiCHECK2/circPAN3-mut153 or cotransfection of miR-183-5p mimic and psiCHECK2/circPAN3-mut183. **(C,D)** Relative luciferase activities analyzed in 293T cells upon cotransfection of miR-153-5p mimic and luciferase reporter psiCHECK2/*XIAP* 3′-UTR-mut153 or cotransfection of miR-183-5p mimic and psiCHECK2/*XIAP* 3′-UTR-mut183. Upregulation of miR-153-5p or miR-183-5p by mimic transfection significantly decreased luciferase activity of WT control reporters, but not the reporters containing circPAN3 or XIAP 3′-UTR sequences with mutated binding sites for miR-153-5p or miR-183-5. Data are presented as means ± SD ($n = 3$). $^{*}p < 0.05$ and $^{**}p < 0.01$ compared with WT control; $^{\#}p < 0.05$ and $^{\#\#}p < 0.01$ compared with miR-153-5p or miR-183-5p mimics.

specific inhibitors, the impact of downregulation of circPAN3 on XIAP expression was counteracted (Figure 5B). Furthermore, downregulation of circPAN3 increased the ratios of CL Cas-3/pro-Cas-3 and CL Cas-9/pro-Cas-9, but this effect was also significantly diminished by cotransfection of circPAN3 siRNA and miR-153-5p or miR-183-5p inhibitors (Figure 5B and Supplementary Figures E3A and E3B, online only, available at www.exphem.org). To verify the role of circPAN3–miR-153-5p/miR-183-5p–XIAP axis in primary AML cells, we repeated the experiment in leukemic cells from five relapsed AML patients and observed similar findings (Figure 5C).

To confirm the interactions between circPAN3 and miR-153-5p/miR-183-5p, we performed a luciferase assay in 293T cells upon cotransfection of miR-153-5p mimic and luciferase reporter psiCHECK2/circPAN3-mut153 or cotransfection of miR-183-5p mimic and psiCHECK2/circPAN3-mut183. As shown in Figures 6A and 6B, upregulation of miR-153-5p or miR-183-5p by mimic transfection could remarkably reduce the luciferase activity of WT reporter. However, this was not the case for the reporters with mutated binding sites for miR-153-5p or miR-183-5, suggesting that miR-153-5p and miR-183-5p interact with circPAN3 via the complementary seed region. A similar assay was performed to confirm the interactions between

miR-153-5p/miR-183-5p and XIAP. As depicted in Figures 6C–6D, upregulation of miR-153-5p or miR-183-5p by mimic transfection significantly decreased the luciferase activity of the WT vector, but not the reporters containing the *XIAP* 3′-UTR with mutated binding sites for miR-153-5p or miR-183-5. Collectively, these findings show that circPAN3 may contribute to ADM resistance in THP-1/ADM cells via the circPAN3–miR-153-5p/miR-183-5p–XIAP axis.

Discussion

Generally, chemoresistant AML cells have distinct molecular and cytogenetic characteristics that lead to deficiencies or perturbations in multiple pathways associated with resistance [25]. Accumulating evidence has suggested that circRNAs are important players in these cellular processes, which act as modulators of gene expression at the transcriptional or posttranscriptional level through interactions with miRNAs or binding to RNA-associated proteins to form RNA–protein complexes [26]. circRNAs appear to be more often downregulated in tumor tissue than in normal tissue [27]. However, recent studies have revealed that chromosomal translocations in cancer generate aberrant fusion circRNAs, which are highly correlated with evolvement of drug resistance [28]. In this study, using high-throughput circRNA microarray, we compared the expression profiles of circRNAs between drug-resistant THP-1/ADM cells and naive THP-1 cells. We found a total of 49 circRNAs expressed significantly differentially between the two cell lines, evidencing the involvement of circRNAs in the development of chemoresistance in AML cells. In the top 10 upregulated circRNAs, circPAN3 attracted our attention due to the increasingly recognized role of its corresponding gene *PAN3* in AML.

A recent study has reported that the gene *PAN3* is considered a candidate gene located in amplified chromosome regions in AML patients with a complex karyotype [21]. In a myelodysplastic syndrome patient that evolved into AML, a fusion of *PAN3* with the gene *PSMA2* was formed from a chromosome translocation [29], suggesting a potential association between the *PAN3* gene and AML development. As further evidence addressing the role of *PAN3* in AML, our in vitro experiments found that downregulation of circPAN3 by siRNA considerably increased the sensitivity of drug-resistant THP-1/ADM cells to ADM; however, after histopathological examination, a significantly higher expression level of circPAN3 was observed in the BM samples from refractory/recurrent AML patients. As mentioned above, chromosomal translocations in cancer contribute to production of aberrant fusion circRNAs, so we assume that the upregulation of circPAN3 in THP-1/ADM cells or AML BM tissues might be attributed to chromosomal translocations that occurred in response to the stress induced by chemotherapeutic drugs. Nevertheless, we still do not know if the circPAN3 identified from THP-1/ADM cells and the BM samples of AML patients was a fusion form. In addition, with PCR sequencing, we examined the chromosomal region where circPAN3 is located (q12.2 chr13) in THP-1/ADM cells and did not find any amplification of this region, suggesting that the enhanced expression of circPAN3 in this cell line is not caused by chromosomal amplification. Therefore, the molecular mechanisms underlying circPAN3 upregulation require further studies.

For the interaction of circRNAs with miRNA, the competitive binding to MREs to relieve inhibitory effects on associated target genes has been regarded as the main mechanism of action [30–32]. In the present study, we predicted the downstream miRNAs of circPAN3 based on conserved seed sequence matches using TargetScan and miRanda and 10 candidates with top mirSVR scores were identified. Of these miRNA candidates, a few have been demonstrated to be involved in a variety of hematologic malignancies and solid tumors. For example, a previous study has reported that expression of miR-153-3p was lower in melanoma tissues and melanoma cells compared with the paratumor tissue and normal melanocytes, whereas overexpression of miR-153-3p could inhibit cell proliferation and invasion and at the same time promote cell apoptosis [33]. Regarding miR-183, its expression has been found to be significantly increased in the BM and serum of pediatric AML patients and serves as an independent prognostic factor for recurrence and survival [34]. A mechanistic study further demonstrated that overexpression of miR-183 significantly enhanced cell proliferation and G_1/S conversion and inhibited apoptosis of leukemia cells [34]. In this study, GO and KEGG analyses identified the downstream genes regulated by these candidate miRNAs. Interestingly, most of these genes are implicated in diverse essential cellular functions, but in cancer cells, these genes are also involved in several aberrant signaling pathways and consequently confer chemoresistance [35–37]. In the circPAN3–miRNA–mRNA interaction network, we found that XIAP, a crucial anti-apoptotic protein, was targeted by both miR-153-5p and miR-183-5p, suggesting that it might be a key downstream molecule regulated by circPAN3.

XIAP belongs to the inhibitor-of-apoptosis proteins (IAPs) that represent a family of endogenous caspase inhibitors [38]. It is the only IAP member that can directly inhibit the activity of the three most important effector caspases, Cas-3, Cas-7, and Cas-9 [39,40]. Recently, numerous studies have revealed that XIAP is regulated by miRNAs at the posttranscriptional level

[41,42]. Particularly, in a wide range of cancer cells, the interactions between the XIAP mRNA and some specific miRNAs potentially overcome drug resistance through interfering with the anti-apoptotic activity of XIAP [43,44]. In this study, we found that downregulation of circPAN3 by siRNA only affects the protein expression of XIAP in THP-1/ADM cells. This finding indicates a posttranscriptional regulation mechanism of circPAN3 on XIAP in which miRNA serves as a connecting link between the two molecules. Regarding the two miRNA candidates identified from the interaction network, their mimics could decrease the expression of XIAP in the ADM-resistant THP-1 cells. Further experiments indicated that siRNA-mediated downregulation of circPAN3 led to a decrease in XIAP protein level, but not in the mRNA level. Strikingly, this effect could be counteracted by specific inhibitors of miR-153-5p and miR-183-5p. Based on these findings, it could be inferred that circPAN3 is most likely responsible for ADM resistance in THP-1/ADM cells via the circPAN3−miR-153-5p/miR-183-5p−XIAP axis. The underlying mechanism might depend on a process in which circPAN3 acts as a "sponge" to sequester miR-153-5p and miR-183-5p, which may block the between both miRNA molecules and the noncoding UTR of *XIAP* mRNA, consequently enhancing transcription of XIAP protein. The luciferase reporter assays revealed that circPAN3 and the 3′-UTR of *XIAP* may share the same miR-153-5p/miR-183-5p response elements in which competitive binding to miR-153-5p and miR-183-5p might exist. However, further studies are needed to confirm this postulation.

Several limitations should be addressed here regarding this study: 1. the small sample size in microarray analysis may decrease statistical power, 2. we only utilized one AML cell line and 42 patient samples, so the results need to be validated in other AML cell lines and on larger numbers of clinical samples, and 3. heterogeneity in the study population may introduce an additional bias in histopathological examination.

In conclusion, we have for the first time to our knowledge generated profiles of differentially expressed circRNAs between chemosensitive and chemoresistant AML cells. We also identified a key circRNA molecule, circPAN3, which may play a crucial role in mediating the development of drug resistance. Our findings provide evidence that circPAN3 can be a valuable indicator for predicting clinical efficacy of chemotherapy in AML patients and also can serve as a potential target for reversing drug resistance in AML.

Acknowledgments

This work was supported by grants from the Young and Middle-Aged Talents Training Projects subsidized by Fujian Provincial Health and Family Planning Commission, Fujian, China (2016-ZQN-5) and the Natural Science Foundation of Fujian Province, Fujian, China (2018J01259).

Conflict of interest disclosure

The authors declare no competing financial interests.

References

1. Siegel R, Ma J, Zou Z, Jemal A. Cancer statistics, 2014. CA Cancer J Clin. 2014;64:9–29.
2. DeSantis CE, Siegel RL, Sauer AG, et al. Cancer statistics for African Americans, 2016: Progress and opportunities in reducing racial disparities. CA Cancer J Clin.. 2016;66:290–308.
3. Orlowski RJ, Mangan JK, Luger SM. Approach to patients with primary refractory acute myeloid leukemia. Curr Opin Hematol. 2015;22:97–107.
4. Du Y, Chen B. Detection approaches for multidrug resistance genes of leukemia. Drug Des Devel Ther. 2017;11:1255–1261.
5. Majidinia M, Yousefi B. Long non-coding RNAs in cancer drug resistance development. DNA Repair (Amst). 2016;45:25–33.
6. Warner JR. The economics of ribosome biosynthesis in yeast. Trends Biochem Sci. 1999;24:437–440.
7. Salmena L, Poliseno L, Tay Y, Kats L, Pandolfi PP. A ceRNA hypothesis: the Rosetta Stone of a hidden RNA language? Cell. 2011;146:353–358.
8. Suzuki H, Tsukahara T. A view of pre-mRNA splicing from RNase R resistant RNAs. Int J Mol Sci. 2014;15:9331–9342.
9. Salzman J, Chen RE, Olsen MN, Wang PL, Brown PO. Cell-type specific features of circular RNA expression. PLoS Genet. 2013;9:e1003777.
10. Memczak S, Jens M, Elefsinioti A, et al. Circular RNAs are a large class of animal RNAs with regulatory potency. Nature. 2013;495:333–338.
11. Hansen TB, Kjems J, Damgaard CK. Circular RNA and miR-7 in cancer. Cancer Res. 2013;73:5609–5612.
12. Bachmayr-Heyda A, Reiner AT, Auer K, et al. Correlation of circular RNA abundance with proliferation−exemplified with colorectal and ovarian cancer, idiopathic lung fibrosis, and normal human tissues. Sci Rep. 2015;5:8057.
13. Wang X, Zhang Y, Huang L, et al. Decreased expression of hsa_circ_001988 in colorectal cancer and its clinical significances. Int J Clin Exp Pathol. 2015;8:16020–16025.
14. Li P, Chen S, Chen H, et al. Using circular RNA as a novel type of biomarker in the screening of gastric cancer. Clin Chim Acta. 2015;444:132–136.
15. Su H, Lin F, Deng X, et al. Profiling and bioinformatics analyses reveal differential circular RNA expression in radioresistant esophageal cancer cells. J Transl Med. 2016;14:225.
16. Xie H, Ren X, Xin S, et al. Emerging roles of circRNA_001569 targeting miR-145 in the proliferation and invasion of colorectal cancer. Oncotarget. 2016;7:26680–26691.
17. Gao D, Zhang X, Liu B, et al. Screening circular RNA related to chemotherapeutic resistance in breast cancer. Epigenomics. 2017;9:1175–1188.
18. O'Donnell MR, Tallman MS, Abboud CN, et al. Acute Myeloid Leukemia, Version 3.2017, NCCN Clinical Practice Guidelines in Oncology. J Natl Compr Canc Netw. 2017;15:926–957.
19. Schmittgen TD, Livak KJ. Analyzing real-time PCR data by the comparative C(T) method. Nat Protoc. 2008;3:1101–1108.
20. Ohmura M, Hishiki T, Yamamoto T, et al. Impacts of CD44 knockdown in cancer cells on tumor and host metabolic systems revealed by quantitative imaging mass spectrometry. Nitric Oxide. 2015;46:102–113.

21. Mrózek K. Cytogenetic, molecular genetic, and clinical characteristics of acute myeloid leukemia with a complex karyotype. Semin Oncol. 2008;35:365–377.
22. Kulcheski FR, Christoff AP, Margis R. Circular RNAs are miRNA sponges and can be used as a new class of biomarker. J Biotechnol. 2016;238:42–51.
23. Shaffer BC, Gillet JP, Patel C, Baer MR, Bates SE, Gottesman MM. Drug resistance: still a daunting challenge to the successful treatment of AML. Drug Resist Updat. 2012;15:62–69.
24. Prabhu KS, Siveen KS, Kuttikrishnan S, et al. Targeting of X-linked inhibitor of apoptosis protein and PI3-kinase/AKT signaling by embelin suppresses growth of leukemic cells. PLoS One. 2017;12:e0180895.
25. Gabra MM, Salmena L. microRNAs and acute myeloid leukemia chemoresistance: a mechanistic overview. Front Oncol. 2017;7:255.
26. Huang C, Shan G. What happens at or after transcription: Insights into circRNA biogenesis and function. Transcription. 2015;6:61–64.
27. Greene J, Baird AM, Brady L, et al. Circular RNAs: biogenesis, function and role in human diseases. Front Mol Biosci. 2017;4:38.
28. Guarnerio J, Bezzi M, Jeong JC, et al. Oncogenic role of fusion-circRNAs derived from cancer-associated chromosomal translocations. Cell. 2016;165:289–302.
29. Panagopoulos I, Gorunova L, Andersen HK, et al. PAN3-PSMA2 fusion resulting from a novel t(7;13)(p14;q12) chromosome translocation in a myelodysplastic syndrome that evolved into acute myeloid leukemia. Exp Hematol Oncol. 2018;7:7.
30. Hansen TB, Jensen TI, Clausen BH, et al. Natural RNA circles function as efficient microRNA sponges. Nature. 2013;495:384–388.
31. Kefas B, Godlewski J, Comeau L, et al. microRNA-7 inhibits the epidermal growth factor receptor and the Akt pathway and is down-regulated in glioblastoma. Cancer Res. 2008;68:3566–3572.
32. Jeck WR, Sorrentino JA, Wang K, et al. Circular RNAs are abundant, conserved, and associated with ALU repeats. RNA. 2013;19:141–157.
33. Zeng HF, Yan S, Wu SF. MicroRNA-153-3p suppress cell proliferation and invasion by targeting SNAI1 in melanoma. Biochem Biophys Res Commun. 2017;487:140–145.
34. Wang X, Zuo D, Yuan Y, Yang X, Hong Z, Zhang R. MicroRNA-183 promotes cell proliferation via regulating programmed cell death 6 in pediatric acute myeloid leukemia. J Cancer Res Clin Oncol. 2017;143:169–180.
35. Brunen D, Willems SM, Kellner U, Midgley R, Simon I, Bernards R. TGF-beta: an emerging player in drug resistance. Cell Cycle. 2013;12:2960–2968.
36. Jiang BH, Liu LZ. Role of mTOR in anticancer drug resistance: perspectives for improved drug treatment. Drug Resist Updat. 2008;11:63–76.
37. Arteaga CL, Engelman JA. ERBB receptors: from oncogene discovery to basic science to mechanism-based cancer therapeutics. Cancer Cell. 2014;25:282–303.
38. Yang YL, Li XM. The IAP family: endogenous caspase inhibitors with multiple biological activities. Cell Res. 2000;10:169–177.
39. Deveraux QL, Takahashi R, Salvesen GS, Reed JC. X-linked IAP is a direct inhibitor of cell-death proteases. Nature. 1997;388:300–304.
40. Eckelman BP, Salvesen GS. The human anti-apoptotic proteins cIAP1 and cIAP2 bind but do not inhibit caspases. J Biol Chem. 2006;281:3254–3260.
41. Heider T, Mutschelknaus L, Radulović V, et al. Radiation induced transcriptional and post-transcriptional regulation of the hsa-miR-23a∼27a∼24-2 cluster suppresses apoptosis by stabilizing XIAP. Biochim Biophys Acta Gene Regul Mech. 2017;1860:1127–1137.
42. Chen P, He YH, Huang X, et al. MiR-23a modulates X-linked inhibitor of apoptosis-mediated autophagy in human luminal breast cancer cell lines. Oncotarget. 2017;8:80709–80721.
43. An X, Sarmiento C, Tan T, Zhu H. Regulation of multidrug resistance by microRNAs in anti-cancer therapy. Acta Pharm Sin B. 2017;7:38–51.
44. Riquelme I, Letelier P, Riffo-Campos AL, Brebi P, Roa JC. Emerging role of miRNAs in the drug resistance of gastric cancer. Int J Mol Sci. 2016;17:424.

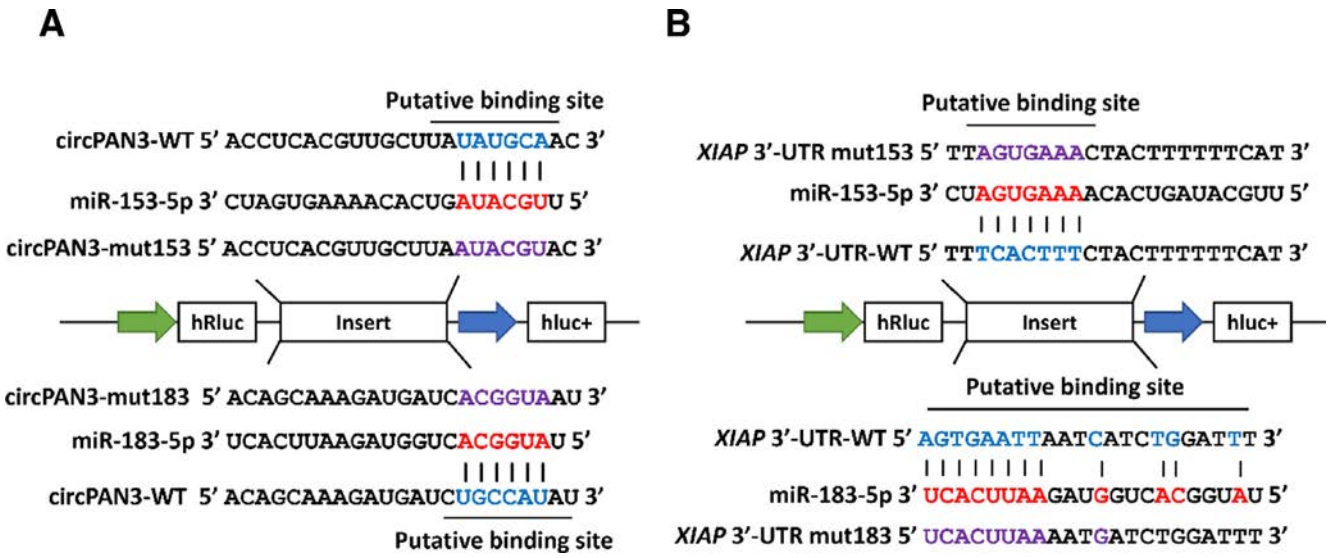

Supplementary Figure 1. (A) Schematic of luciferase reporters containing wild-type (WT) and mutant sequences of circPAN3 (circPAN3-mut153 and cirPAN3-mut183). (B) Schematic of luciferase reporters containing WT and mutant sequences of the 3′-untranslated region (3′-UTR) of *XIAP*.

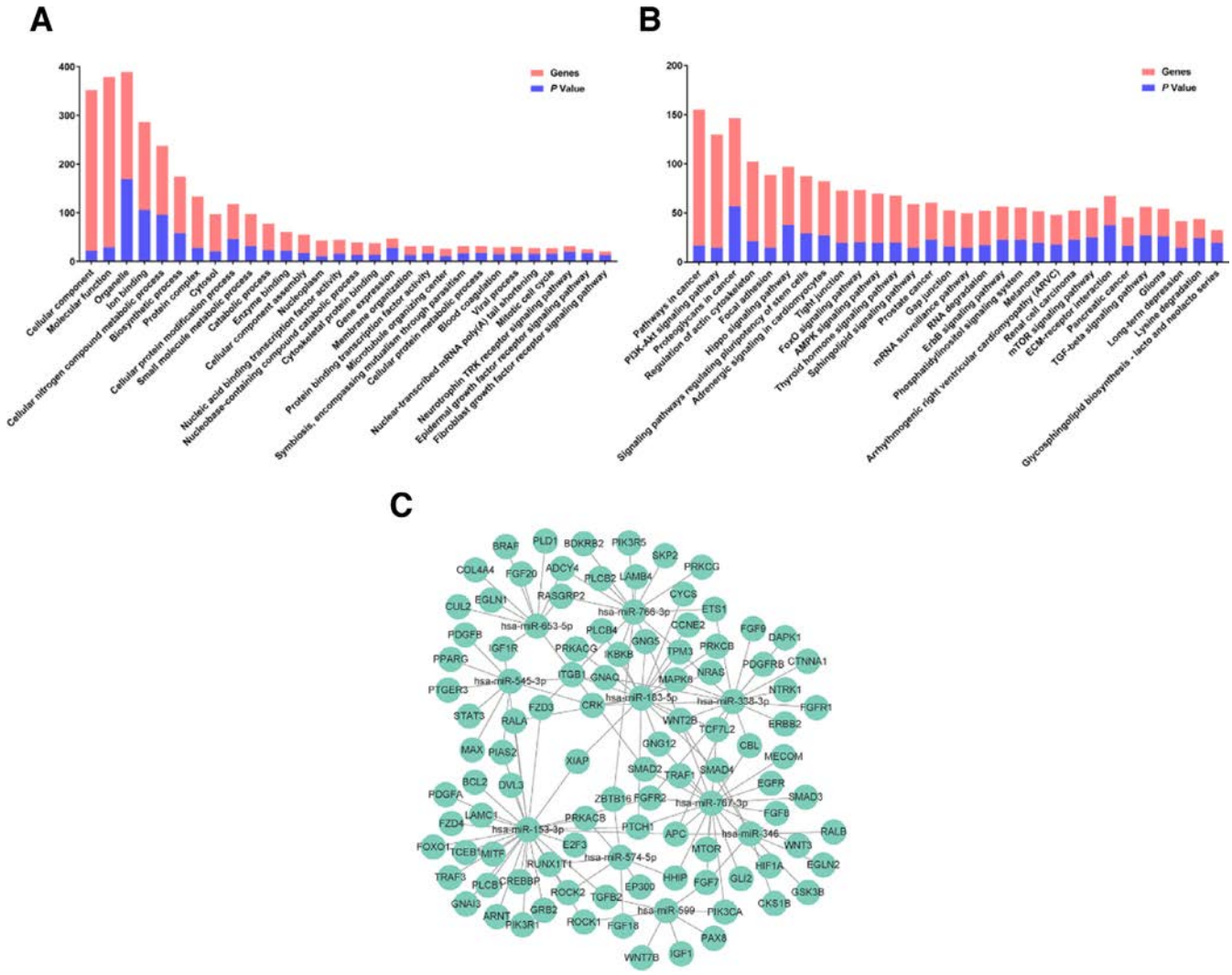

Supplementary Figure 2. Prediction of target genes and miRNAs, and bioinformatic analysis. (A) GO enrichment analysis of target genes corresponding to circPAN3. (B) KEGG pathway analysis of target genes involved in circPAN3 related pathways. (C) The interaction network of circPAN3 and its co-expressed genes and target miRNAs. The panorama network consists of circPAN3 and its target genes and ten miRNAs based on seed sequence pairing interactions.

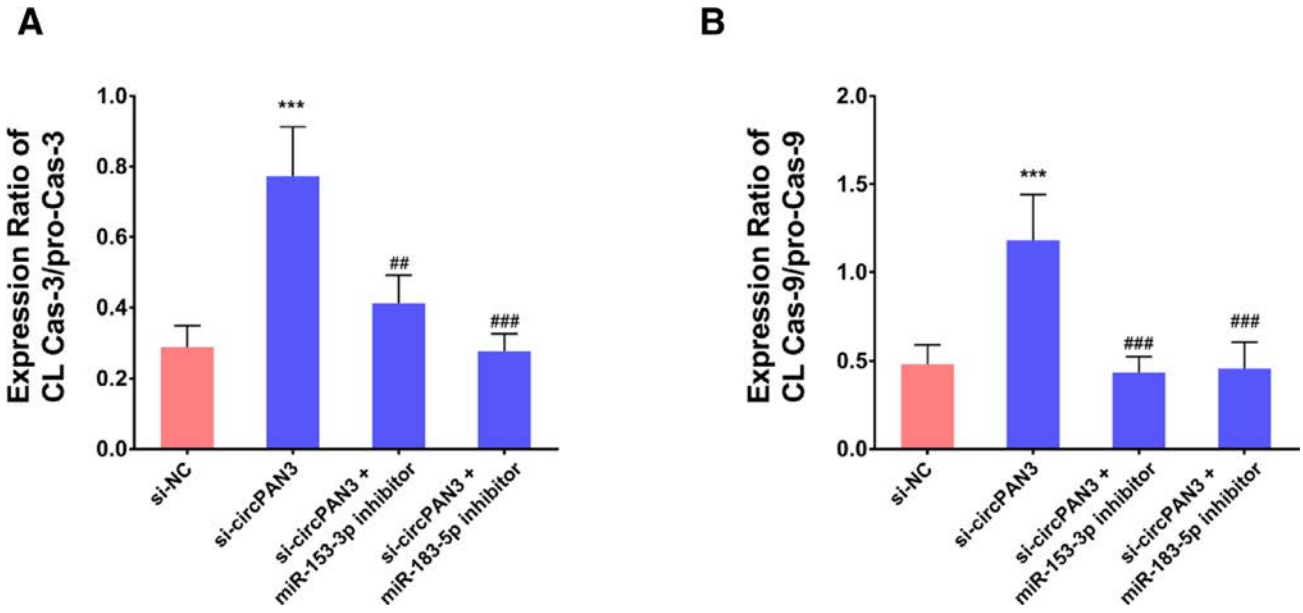

Supplementary Figure 3. Panels (A) and (B) show that circPAN3 down-regulation by specific siRNA significantly increased the ratios of CL Cas-3/pro-Cas-3 and CL Cas-9/pro-Cas-9 in THP-1/ADM cells. However, this effect was counteracted by co-transfection either miR-153-5p or miR-183-5p specific inhibitors. The protein levels were determined by Western blot, and β-actin served as an internal control. Data are presented as means ± SD (n = 5). $^{***}P < 0.001$ compared with miR-NC; $^{\#\#}P < 0.01$ and $^{\#\#\#}P < 0.001$ compared with si-circPAN3.